Pressure-Modulated Broadband Emission in 2D Layered Hybrid Perovskite-Like Bromoplumbate

Verónica Gómez, Svetlana Klyatskaya, Olaf Fuhr, Sergii Kalytchuk, Radek Zbořil, Manfred Kappes, Sergei Lebedkin, and Mario Ruben*

ABSTRACT: Two dimensional (2D) layered hybrid bromoplumbate perovskites are promising candidates for solution processed light emitting materials. Here, we report the synthesis and characterization of two novel layered bromoplumbates: $(4BrPhMA)_2PbBr_4$ (**1**) and $(4BrPhA)_6Pb_3Br_{12}$ (**2**), where 4BrPhMA is (4 bromophenyl)methylammonium and 4BrPhA is (4 bromophenyl) ammonium. Despite similar optical absorption, these materials show remarkably different photoluminescence properties: **1** emits a narrow exciton band at ca. 395 nm with a very small bandwidth (particularly at low temperatures of 15−50 K) and Stokes shift, while **2** exhibits a broad emission at ca. 560 nm with a large Stokes shift, both at low and ambient temperatures. However, under several kbar of hydrostatic pressure, the broad emission diminishes and a new band reversibly develops at ca. 395 nm, similar to that in **1**. Our results emphasize organic layer flexibility as an important design factor for this class of perovskite like materials featuring broadband emission.

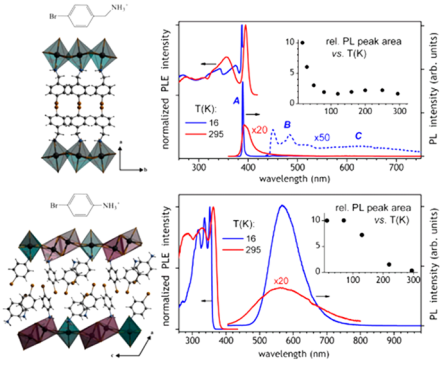

INTRODUCTION

Organic−inorganic hybrid lead halide perovskites have attracted much attention since $CH_3NH_3PbX_3$ (X: halide) was used for the first time as light absorber for solar cells, which presently reach conversion efficiencies of up to 22.7%.[1−5] In addition to photovoltaic applications, hybrid perovskites are potentially suitable for other optoelectronic and photonic devices such as photodetectors, waveguides, lasers, and light emitting diodes.[6,7] The optical and electrical properties of these materials are mainly determined by the dimensionality and geometry of their inorganic framework. The organic cation, however, can modify this framework and thereby alter and tune the optoelectronic characteristics.[8,9] For instance, alkyl or aryl ammonium cations usually lead to formation of 2D layered perovskites with a general formula A_2PbX_4 (A: monovalent organic cation, X: Cl, Br, and I),[10−16] which consist of (001) oriented lead halide semiconductor sheets placed between organic insulating layers. The layered configuration naturally results in 2D charge confinement. Excitons confined in the inorganic layer demonstrate large binding energies enhanced through a dielectric confinement effect[17] and display typical narrow band free exciton photo luminescence (PL).[16,18] In contrast, a broad (in some cases white light), lower energy emission has also been observed recently for a few 2D layered lead halide systems.[19−27] Although only moderate emission efficiencies have been reported thus far, these systems have immediately attracted attention, as white light phosphors are rare.[28] A general feature of such lead halide perovskites is a "distorted", e.g., (110) corrugated, arrangement of the inorganic layers, which correlates with the emission properties.[26] However, the broad emission has also been observed at low temperatures in the "usual" (001) lead halide systems.[23,29]

Here, we report the synthesis and characterization of two new 2D layered perovskite compounds with structurally close organic cations: $(4BrPhMA)_2PbBr_4$ (**1**) and $(4BrPhA)_6Pb_3Br_{12}$ (**2**) (4BrPhMA: (4 bromophenyl) methylammonium, 4BrPhA: (4 bromophenyl)ammonium, Figure 1a,b). These compounds demonstrate that a small variation of the cation can result in notably distinct organic−inorganic layer arrangements and fundamentally different optical properties. **1** mainly displays narrow violet emission due to free excitons, while **2** only shows a broad, low energy emission covering a large part of the visible spectrum. Interestingly, the PL properties of **2** change dramatically and reversibly under a few kbar hydrostatic pressure: The broad emission blue shifts and strongly diminishes, whereas the free exciton emission (similar to that in **1**) appears.

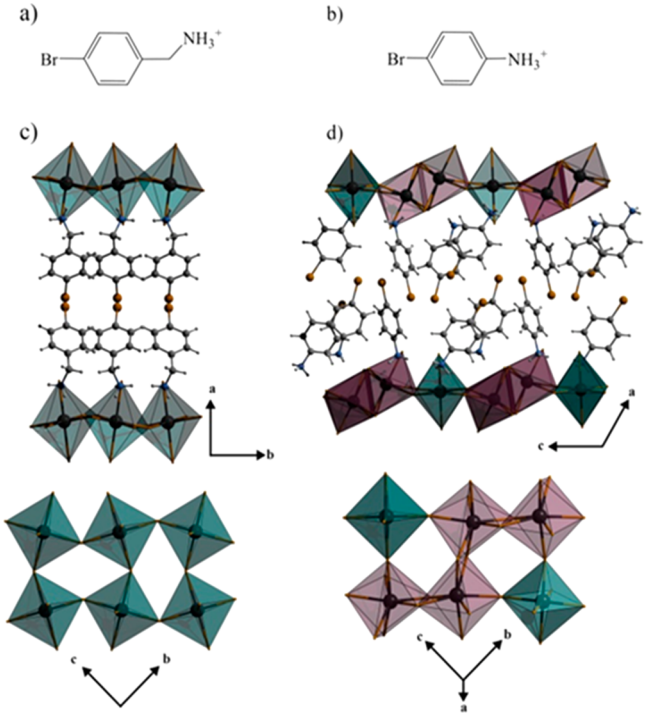

Figure 1. Structures of (4 bromophenyl)methylammonium (4BrPhMA) (a) and (4 bromophenyl)ammonium (4BrPhA) (b); crystal structures of compounds **1** $(4BrPhMA)_2PbBr_4$ (c) and **2** $(4BrPhA)_6Pb_3Br_{12}$ (d). Dark gray, yellow, blue, and light gray atoms represent Pb, Br, N, and C, respectively. Green and pink polyhedra correspond to $PbBr_6$ and $PbBr_7$ units, respectively.

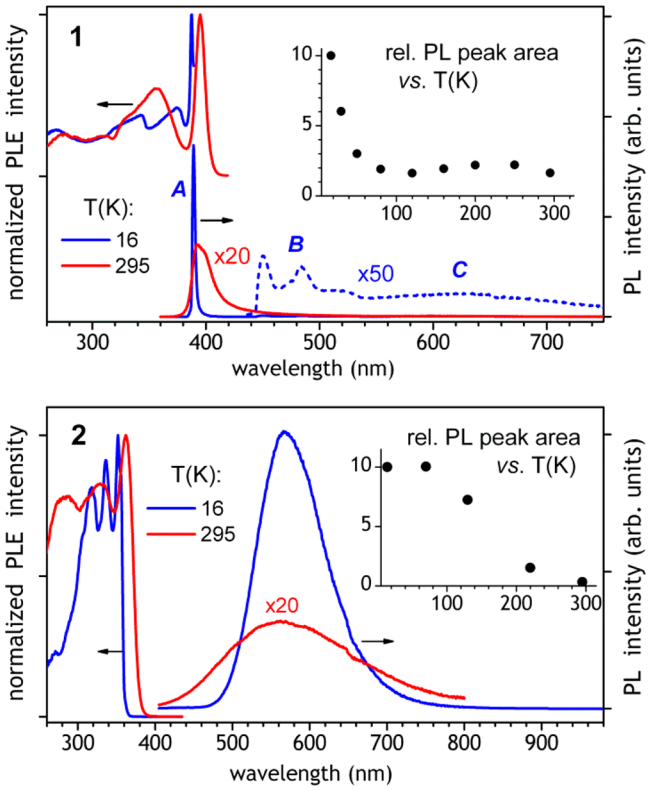

Figure 2. Photoluminescence emission (PL) and excitation (PLE) spectra of compounds **1** and **2** at low (16 K) and ambient (295 K) temperatures. The PL/PLE spectra were excited/recorded at 330/392 nm (330/440 nm at 295 K) and 320/560 nm for **1** and **2**, respectively. The inserts show the relative integral PL intensity vs temperature. The PLE spectra of **1** are vertically shifted for clarity.

RESULTS AND DISCUSSION

1 crystallizes in the centrosymmetric orthorhombic space group *Pccn*. The crystal structure shows the usual 2D periodic arrangement of single inorganic sheets formed by (001) oriented, corner sharing, quite regular $PbBr_6$ octahedra and separated by organic double layers (Figures 1c and S1 and Table S1). However, **2** crystallizes in the centrosymmetric monoclinic space group $P2_1/c$, and the crystal structure consists of alternate double 4BrPhA layers and inorganic single layers formed by slightly distorted octahedral $PbBr_6$ units and capped octahedral $PbBr_7$ units (Figures 1d and S2 and Table S2). Each $PbBr_6$ unit (green polyhedra) is linked to four $PbBr_7$ units (pink polyhedra) in a corner sharing fashion. This arrangement is unusual and, to our knowledge, has not been reported previously. Unit cell parameters for both compounds are given in Table S3. The distinct coordination patterns of the inorganic layers are reflected by the different Raman spectra of **1** and **2** in the low frequency region of ~10−90 cm^{-1} (Figure S3). This region of strong Raman signals is associated with contributions of vibrational modes of PbBr units.[30] In comparison, the Raman spectra within ~200−2000 cm^{-1}, mostly contributed by the organic layers, look rather similar (Figure S3).

The absorption spectra of both materials measured as crystalline powders in an integrating sphere (Figure S4) resemble those of the previously reported 2D lead bromide perovskites.[11,15,16,30] The bandgaps estimated from the onset of absorption are 3.1 and 3.3 eV for **1** and **2**, respectively.

Despite the similar absorption, **1** and **2** show strikingly different PL (Figures 2 and S5−S9). Under UV photo excitation, **2** displays a broad (0.77 eV fwhm) visible emission centered at 560 nm (2.21 eV) under ambient conditions. The Commission Internationale de l'Eclairage (CIE) chromaticity coordinates (0.38, 0.45) of this emission are depicted in Figure S9 and show a larger contribution from the green region as compared to white light. By decreasing the temperature down to 16 K, the emission maximum slightly shifts to 568 nm and the bandwidth reduces to 0.37 eV. Similar to **1**, the PLE spectra of **2** show a narrow band at the edge of absorption at 353/363 nm (3.51/3.42 eV) at 16/295 K, which may also be attributed to excitons in the inorganic layer of **2**. However, no corresponding sharp excitonic emission (like *A* in **1**, see below) could be detected, indicating that this relaxation channel is inefficient in **2**. The PL quantum yield of the broad emission at ambient temperature was determined as 1.5 and 3.2% when excited at 330 and 370 nm, respectively. The former value increases, however, to ~50% below 100 K, as can be estimated from the temperature dependence in Figure 2. Interestingly, the PL lifetime of **2** dramatically depends on the temperature, increasing from 10 *ns* at 295 K to 4.5 *μs* at 14 K (Figure S8).

In contrast, **1** emits violet light as a narrow band (denoted as *A* in Figure 2) at about 395 nm (3.14 eV). A counterpart band at the edge of the PL excitation (PLE) spectrum is also narrow and overlaps the emission, demonstrating a very small Stokes shift. These features become particularly sharp at low temperatures: at T = 16 K the PLE and PL bands peak at 387.5 and 389.5 nm, respectively, corresponding to a Stokes shift of *ca.* 15 meV. The emission line width (FWHM) at T ~ 15−50 K is about 2 nm (15 meV). Such a small line width, measured on a powder sample, indicates a high degree of

crystallinity. All these features are characteristic for free 2D excitons which are photogenerated in the inorganic layers of **1**. This behavior is analogous to numerous other (100) oriented 2D bromoplumbates.[8,11,13,16,18] By increasing the temperature to 295 K, the emission of **1** redshifts to ca. 395 nm, decreases in the integral intensity by a factor of 5, and significantly broadens up to *ca.* 150 meV (FWHM). We attribute the latter to mostly inhomogeneous broadening. It is also evidenced by changes in the shape of the exciton PL and PLE bands by varying, respectively, the excitation and emission wavelengths close to these bands. The PL quantum yield for **1** under ambient conditions and excitation at 357 nm was determined to be 2.1%.

Besides the major sharp emission *A*, **1** also shows a vibronically structured band *B* at ~480 nm (only observed below ~50 K) and a broad band *C* at ~600 nm (especially pronounced below ~100 K). The absolute intensities of *B* and *C* at T = 16 K are by a factor of 300−500 lower than that of *A*. In contrast, the integral intensity of these broad emissions is not negligible and amounts to ca. 15% of the value for the sharp band A at 16 K. The PLE spectra corresponding to *B* and *C* resemble that of *A* but demonstrate a strongly reduced exciton band at the edge of absorption (Figure S5). Different origins of *A*, *B*, and *C* are further evidenced by their decay kinetics under pulsed UV laser excitation. As typical for free exciton PL, emission *A* decays fast, within nanoseconds (both at low and ambient temperatures), whereas *C* and *B* decay on the time scale of a few and hundreds of microseconds, respectively (Figure S7). Two frequencies of ~1050 and 1550 cm^{-1} can be roughly estimated from the vibration progression of *B*, indicating coupling to vibrations of the organic cation. We tentatively assign emission *B* to triplet excitons in the organic layer of **1**. They may be generated either by UV excitation of the organic cation or via energy transfer from the inorganic layer. Emission *C* might have a similar origin as the broad emission of **2** described above. Additional information on the correlation between PL and structure can be delivered by high pressure experiments. Figures 3 and S10 present PLE

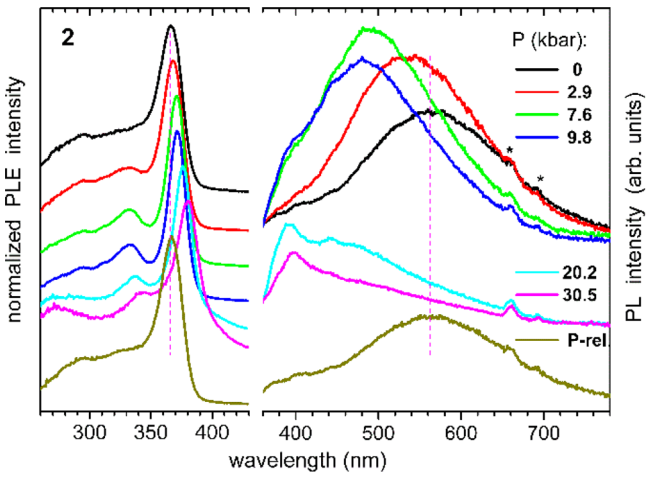

Figure 3. PL spectra of **2** in a diamond anvil cell at ambient temperature. Emission was excited at 330 nm and the excitation spectra were recorded at 550 (until 2.9 kbar), 500 (until 20.2 kbar), 480 (30.5 kbar), and 550 nm (pressure release). The spectra are vertically shifted for convenience. The asterisks denote the residual second order excitation line and ruby emission at 660 and 694 nm, respectively. For comparison with **1**, see Figure S10.

and PL spectra of **1** and **2** measured at ambient temperature in a diamond anvil cell up to *ca.* 20 and 30 kbar pressure, respectively (for details see the Supporting Information). Referring to high pressure studies on comparable 2D hybrid perovskites, no phase transition but only compression, mostly of the organic layers, are expected under such relatively moderate pressures.[31] Both exciton PLE and PL bands of **1** demonstrate a moderate linear redshift of *ca.* (5−6 meV/kbar) up to 10 kbar (Figure S11). This shift is consistent with those observed for other 2D and 3D perovskites in the low pressure regime. Emission broadening and a strong intensity decrease accompany a further rise of pressure. The PL only recovers to about 10% of the initial intensity after release of 19 kbar pressure (Figure S10). This indicates structural degradation of the inorganic layer in **1** under relatively moderate pressure. In contrast, the broadband emission of **2** at 560 nm shows a linear blueshift of as much as +45 meV/kbar up to 10 kbar pressure (Figure S11) and thereby increases in intensity by a factor of 1.5. More interestingly, a further rise of pressure results in reduction and flattening of the (blueshifted) broad emission and development of a new PL band at ca. 395 nm. Its shift under pressure follows that of the photoluminescence excitation (PLE) exciton band which linearly redshifts at ca. −4 meV/kbar up to 30.5 kbar (the highest pressure probed). Consequently, the new PL band can be assigned to exciton emission. Applying moderate hydrostatic pressure to **2** apparently strongly affects (elevates in energy and suppresses), the deep state(s) producing the broadband visible emission and thus gives rise to the exciton emission at ca. 395 nm, which is missing under normal conditions. After 30.5 kbar pressure release, the PL of **2** recovers almost completely, with the intensity of 70% of the initial value (Figure 3). Importantly, these results evidence that the specific arrangement of the inorganic layer in **2** does not preclude free exciton emission. This arrangement and its interplay with the organic layers rather provide for an additional competing relaxation channel (leading to the broadband low energy emission). The latter is very efficient in **2** under normal conditions but becomes strongly damped under pressure.

As mentioned above, a broad visible emission with a large Stokes shift, similar to that of **2**, has recently been observed for several other 2D lead halide systems.[19−27] Parameters of this emission (spectral position and width, Stokes shift, lifetime, and temperature dependence) differ from one system to the next. It is presently not certain to which extent its mechanism is generic or system dependent. It has been shown that 2D lead halide layers can provide for large deformation potential resulting in self trapping of excitons, i.e., in formation of polarons, with binding energies up to many hundreds of meV.[32−34] The localized polaron midgap states may act as recombination states producing the above emission. This mechanism has been commonly proposed.[19,23,26,27] On the other hand, solution processed lead halide perovskites are well known to be defect rich materials. For some 2D compounds with a moderately (~0.5 eV) Stokes shifted broad emission permanent defects have been considered as related recombination centers.[29,35] In the case of **2**, a candidate mechanism should comply with the experimental observations described above. Namely, the broadband PL is related to a rather deep emissive state(s). Its average depth can be estimated as 1.2−1.3 eV by referring the emission maximum at 2.2 eV to the excitation band at ca. 3.5/3.4 eV (16/295 K) (Figure 2). A visual appearance of **2** (snow white polycrystalline powder,

Figure S2) and its reflection spectrum (no notable absorption within ~500−800 nm, Figure S4) argue for the transient character of those states and against the presence of permanent deep level traps (color centers) at high concentrations. In addition, the dramatic changes in the PL of **2** under moderate hydrostatic pressure suggest PL related structural reorganization. These results strongly suggest self trapping of excitons as the origin of the broadband emission, likely without the assistance of possible structural defects. A further argument for this mechanism is provided by the linear dependence of the emission intensity versus ns pulsed UV laser excitation intensity up to ~3 MW/cm^2 (Figure S12). This measurement was done at T = 20 K, whereby the emission of **2** is a major relaxation channel with the quantum efficiency of ~50% (see above) and relatively long decay time of a few microseconds. A rough estimation shows that the concentration of excitations photogenerated at such laser intensity amounts to ~0.1% of the number of all $PbBr_6$ and $PbBr_7$ units. The observed unsaturated PL in such regime is consistent with self trapping associated with dynamic structural distortions − non limited by defects.

CONCLUSION

In summary, we have synthesized and characterized two novel 2D bromoplumbate perovskite compounds $(4BrPhMA)_2PbBr_4$ (**1**) and $(4BrPhA)_6Pb_3Br_{12}$ (**2**). These related compounds show arrestingly how a small variation of the organic cation (PhMA vs PhA, presence of a $-CH_2-$ group), constituting PL "inactive" organic layers, can modulate the structure and properties of lead halide layers, thus resulting in rather different optoelectronic (PL) properties. **1** shows pronounced and sharp PL excitation and emission bands at ca. 390 nm with a very small Stokes shift, attributed to free excitons in the lead halide layers. The emission linewidth down to *ca.* 15 meV at temperatures below ~50 K, measured on a polycrystalline sample, is unusually small for 2D perovskite compounds, likely indicating a high degree of crystallinity of **1**. In contrast, **2** displays a similar PL excitation band at *ca.* 360 nm, but a broad green white emission at ca. 560 nm with a respectively large Stokes shift. The latter indicates a quite different major relaxation mechanism for photoexcitations in **2** versus **1**. Moreover, the broad emission of **2** decreases, and the free exciton band at ca. 390 nm (similar to that in **1**) reversibly appears under application of a few kbar pressure in diamond anvil cell. The broad emission can be attributed to deep self trapping of excitons associated with (dynamic) structural distortions of the bromoplumbate octahedra. Correspondingly, this emission channel is damped (and the higher energy free exciton emission enabled) under pressure which stiffens the structure of **2**. Our results point to the indirect but important role of the organic layer, namely, its structural flexibility (or stiffness), in development of low energy emissive states in 2D hybrid lead halide perovskites. A consideration of this aspect may be helpful when designing broadband light emitters based on this class of materials.

METHODS

All reagents and solvents were purchased from commercial vendors and used as received without further purification. The reactions were carried out in air.

To synthesize $(4BrPhMA)_2PbBr_4$ (**1**), $PbBr_2$ (0.150 g, 0.409 mmol) was dissolved in 8 mL of HBr (47 wt %) at room temperature. Then (4 bromophenyl)methylammonium chloride (0.182 g, 0.818 mmol) was added, and the mixture was heated until dissolution. After cooling down, transparent crystals were obtained, which were removed by filtration, washed with diethyl ether, and dried in air. Yield: 0.260 g, 71%. Calcd for $C_{14}H_{18}Br_6N_2Pb$ (900.93) (%): C, 18.66; H, 2.01; N, 3.11. Found: C, 18.7; H, 2.0; N, 3.1. EDX analysis indicated a Pb:Br ratio of 1:5.6. Selected IR data (cm^{-1}, KBr): 3445 w, 3089 vs, 3004 vs, 2905 s, 1592 m, 1492 s, 1475 vs, 186 s, 1013 m, 829 vs, 609 w, 519 m.

For $(4BrPhA)_6Pb_3Br_{12}$ (**2**), $PbBr_2$ (0.119 g, 0.325 mmol) was dissolved in 5 mL of HBr at room temperature. Then (4 bromophenyl)amine (0.112 g, 0.650 mmol) was added, and the mixture was heated until dissolution. After cooling down, transparent needlelike crystals were formed, which were removed by filtration, washed with diethyl ether, and dried in air. Yield: 0.148 g, 52%. Calcd for $C_{36}H_{42}Br_{18}N_6Pb_3$ (2618.70) (%): C, 16.51; H, 1.62; N, 3.21. Found: C, 16.47; H, 1.5; N, 3.2. EDX analysis indicated a Pb/Br ratio of 1:5.8. Selected IR data (cm^{-1}, KBr): 3450 w, 2993 s, 2561 m, 1559 m, 1479 vs, 1095 w, 1071 m, 1015 m, 810 s, 480 s.

Infrared spectra were recorded in KBr pellets in the 4000−400 cm^{-1} range with a PerkinElmer Spectrum GX FTIR spectrometer. Elemental analysis of C, H, and N were carried out on a Vario Micro Cube. Energy dispersive X ray (EDX) measurements were carried out on a scanning electron microscope Gemini LEO 1530 with an EDX detector.

Single crystal XRD for compounds **1** and **2** was carried out using a STOE IPDS2T diffractometer with graphite monochromated Mo Kα radiation (λ = 0.71073 Å) at 180 K. Using Olex2,[36] the crystal structures were solved with the SHELXS structure solution program[37] using direct methods and refined with SHELXL refinement package[38] using least squares minimization. H atoms were added at idealized positions on their respective parent atoms. Crystal data and refinement parameters are given in Table S3. CCDC 1571202 and 1571203 contain the crystallographic data for this paper. These data can be obtained free of charge from the Cambridge Crystallographic Data Centre via www.ccdc.cam.ac.uk/conts/retrieving.html.

Raman spectra were acquired on a WITec CRM200 microscope at 633 nm excitation with the optics modified to include low frequency volume holographic grating filters.[39] Absorption spectra were measured at room temperature on a Varian Cary 500 UV−vis−NIR spectrometer with an integrating sphere attachment, using polycrystalline samples dispersed in mineral oil between two quartz plates. PL spectra were recorded ona Horiba JobinYvon Fluorolog 322 spectrometer equipped with double monochromators and a closed cycle optical cryostat (Leybold) operating within a temperature range of 15−300 K. Hamamatsu R9110 and R5509 photomultipliers covered an emission spectral range of ~300−830 and 450−1400 nm, respectively. Samples were prepared in a similar way as for the absorption measurements and mounted on the coldfinger of the cryostat. All emission spectra were corrected for the wavelength dependent response of the spectrometer and detector (in relative photon flux units). The absolute wavelength positions are accurate with this instrument within ±0.5 nm. PL decay traces on the time scale of tens of nanoseconds to milliseconds were acquired by connecting a photomultiplier to a 500 MHz oscilloscope (via a 50 Ohm or larger load, depending on the time scale) and using a nitrogen laser for nanosecond pulsed excitation at 337 nm. Faster decays were measured on a FLS980 fluorescence spectrometer (Edinburgh Instruments) with a time correlated single photon counting (TCSPC) system and a picosecond pulsed excitation laser at 375 nm (EPL 375). This instrument was also used to determine PL quantum yields of **1** and **2** at ambient temperature, using an integrating sphere accessory (Edinburgh Instruments). PL of **1** and **2** under high pressure in a diamond anvil cell was recorded with the Fluorolog 3 spectrometer. These experiments are described in detail in the Supporting Information.

■ ASSOCIATED CONTENT

● Supporting Information

The Supporting Information is available free of charge at https://pubs.acs.org/doi/10.1021/acs.inorgchem.0c01490.

Experimental details (PDF)

Accession Codes

CCDC 1571202 and 1571203 contain the supplementary crystallographic data for this paper. These data can be obtained free of charge via www.ccdc.cam.ac.uk/data request/cif, or by emailing data request@ccdc.cam.ac.uk, or by contacting The Cambridge Crystallographic Data Centre, 12 Union Road, Cambridge CB2 1EZ, UK; fax: +44 1223 336033.

■ AUTHOR INFORMATION

Corresponding Author

Mario Ruben − *Institute of Nanotechnology, Karlsruhe Institute of Technology, 76344 Eggenstein Leopoldshafen, Germany; Institut de Physique et Chimie des Matériaux de Strasbourg, CNRS Université de Strasbourg, Strasbourg CEDEX 2 67034, France;* orcid.org/0000 0002 7718 7016; Email: mario.ruben@kit.edu

Authors

Verónica Gómez − *Institute of Nanotechnology, Karlsruhe Institute of Technology, 76344 Eggenstein Leopoldshafen, Germany*

Svetlana Klyatskaya − *Institute of Nanotechnology, Karlsruhe Institute of Technology, 76344 Eggenstein Leopoldshafen, Germany;* orcid.org/0000 0003 2883 750X

Olaf Fuhr − *Institute of Nanotechnology and Karlsruhe Nano Micro Facility (KNMF), Karlsruhe Institute of Technology, 76344 Eggenstein Leopoldshafen, Germany*

Sergii Kalytchuk − *Regional Centre of Advanced Technologies and Materials Department of Physical Chemistry, Faculty of Science, Palacky University, 78371 Olomouc, Czech Republic;* orcid.org/0000 0002 6371 8795

Radek Zbořil − *Regional Centre of Advanced Technologies and Materials Department of Physical Chemistry, Faculty of Science, Palacky University, 78371 Olomouc, Czech Republic;* orcid.org/0000 0002 3147 2196

Manfred Kappes − *Institute of Nanotechnology and Institute of Physical Chemistry, Karlsruhe Institute of Technology, 76344 Eggenstein Leopoldshafen, Germany;* orcid.org/0000 0002 1199 1730

Sergei Lebedkin − *Institute of Nanotechnology, Karlsruhe Institute of Technology, 76344 Eggenstein Leopoldshafen, Germany*

Complete contact information is available at: https://pubs.acs.org/10.1021/acs.inorgchem.0c01490

Author Contributions

The manuscript was written through contributions of all authors. All authors have given approval to the final version of the manuscript.

Funding

This research was funded by the KIT, Palacky University, DFG, ERDF and Baden Württemberg Stiftung

Notes

The authors declare no competing financial interest.

■ ACKNOWLEDGMENTS

This work was supported by the Deutsche Forschungsgemeinschaft (DFG, TRR 88 "3MET" and SPP 1928 COORNETs), the Karlsruhe Nano Micro Facility (KNMF), the HPC 2 program of the Baden Württemberg Stiftung, the PeroRS and EC MODIGLIANI projects. R.Z. and S.K. acknowledge the support from the Operational Programme Research, Development and Education − European Regional Development Fund, project no. CZ.02.1.01/0.0/0.0/16 019/0000754 of the Ministry of Education, Youth and Sports of the Czech Republic.

■ REFERENCES

(1) Kojima, A.; Teshima, K.; Shirai, Y.; Miyasaka, T. Organometal Halide Perovskites as Visible Light Sensitizers for Photovoltaic Cells. *J. Am. Chem. Soc.* **2009**, *131* (17), 6050−6051.

(2) Im, J. H.; Lee, C. R.; Lee, J. W.; Park, S. W.; Park, N. G. 6.5% Efficient Perovskite Quantum Dot Sensitized Solar Cell. *Nanoscale* **2011**, *3* (10), 4088−4093.

(3) Yang, W. S.; Noh, J. H.; Jeon, N. J.; Kim, Y. C.; Ryu, S.; Seo, J.; Seok, S. I. High Performance Photovoltaic Perovskite Layers Fabricated through Intramolecular Exchange. *Science* **2015**, *348* (6240), 1234−1237.

(4) Yang, S.; Fu, W.; Zhang, Z.; Chen, H.; Li, C. Z. Recent Advances in Perovskite Solar Cells: Efficiency, Stability and Lead Free Perovskite. *J. Mater. Chem. A* **2017**, *5* (23), 11462−11482.

(5) Yang, W. S.; Park, B. W.; Jung, E. H.; Jeon, N. J.; Kim, Y. C.; Lee, D. U.; Shin, S. S.; Seo, J.; Kim, E. K.; Noh, J. H.; et al. Iodide Management in Formamidinium Lead Halide−Based Perovskite Layers for Efficient Solar Cells. *Science* **2017**, *356* (6345), 1376−1379.

(6) Sutherland, B. R.; Sargent, E. H. Perovskite Photonic Sources. *Nat. Photonics* **2016**, *10* (5), 295−302.

(7) Zhang, Y.; Liu, J.; Wang, Z.; Xue, Y.; Ou, Q.; Polavarapu, L.; Zheng, J.; Qi, X.; Bao, Q. Synthesis, Properties, and Optical Applications of Low Dimensional Perovskites. *Chem. Commun.* **2016**, *52* (94), 13637−13655.

(8) Saparov, B.; Mitzi, D. B. Organic−Inorganic Perovskites: Structural Versatility for Functional Materials Design. *Chem. Rev.* **2016**, *116* (7), 4558−4596.

(9) Quarti, C.; Marchal, N.; Beljonne, D. Tuning the Optoelectronic Properties of Two Dimensional Hybrid Perovskite Semiconductors with Alkyl Chain Spacers. *J. Phys. Chem. Lett.* **2018**, *9* (12), 3416−3424.

(10) Calabrese, J.; Jones, N. L.; Harlow, R. L.; Herron, N.; Thorn, D. L.; Wang, Y. Preparation and Characterization of Layered Lead Halide Compounds. *J. Am. Chem. Soc.* **1991**, *113* (6), 2328−2330.

(11) Kitazawa, N. Excitons in Two Dimensional Layered Perovskite Compounds: $(C_6H_5C_2H_4NH_3)_2Pb(Br,I)_4$ and $(C_6H_5C_2H_4NH_3)_2Pb(Cl,Br)_4$. *Mater. Sci. Eng., B* **1997**, *49* (3), 233−238.

(12) Mitzi, D. B. A Layered Solution Crystal Growth Technique and the Crystal Structure of (C6H5C2H4NH3)2PbCl4. *J. Solid State Chem.* **1999**, *145* (2), 694−704.

(13) Mercier, N.; Poiroux, S.; Riou, A.; Batail, P. Unique Hydrogen Bonding Correlating with a Reduced Band Gap and Phase Transition in the Hybrid Perovskites $(HO(CH_2)_2NH_3)_2PbX_4$ (X = I, Br). *Inorg. Chem.* **2004**, *43* (26), 8361−8366.

(14) Billing, D. G.; Lemmerer, A. Synthesis and Crystal Structures of Inorganic−Organic Hybrids Incorporating an Aromatic Amine with a Chiral Functional Group. *CrystEngComm* **2006**, *8* (9), 686−695.

(15) Zhang, S.; Lanty, G.; Lauret, J. S.; Deleporte, E.; Audebert, P.; Galmiche, L. Synthesis and Optical Properties of Novel Organic−Inorganic Hybrid Nanolayer Structure Semiconductors. *Acta Mater.* **2009**, *57* (11), 3301−3309.

(16) Kitazawa, N.; Aono, M.; Watanabe, Y. Excitons in Organic−Inorganic Hybrid Compounds (CnH2n+1NH3)2PbBr4 (N = 4, 5, 7 and 12). *Thin Solid Films* **2010**, *518* (12), 3199−3203.

(17) Ishihara, T.; Hong, X.; Ding, J.; Nurmikko, A. V. Dielectric Confinement Effect for Exciton and Biexciton States in PbI4 Based Two Dimensional Semiconductor Structures. *Surf. Sci.* **1992**, *267* (1), 323−326.
(18) Tanaka, K.; Takahashi, T.; Kondo, T.; Umeda, K.; Ema, K.; Umebayashi, T.; Asai, K.; Uchida, K.; Miura, N. Electronic and Excitonic Structures of Inorganic−Organic Perovskite Type Quan tum Well Crystal (C4H9NH3) 2PbBr4. *Jpn. J. Appl. Phys.* **2005**, *44* (8R), 5923.
(19) Smith, M. D.; Karunadasa, H. I. White Light Emission from Layered Halide Perovskites. *Acc. Chem. Res.* **2018**, *51* (3), 619−627.
(20) Li, Y. Y.; Lin, C. K.; Zheng, G. L.; Cheng, Z. Y.; You, H.; Wang, W. D.; Lin, J. Novel ⟨110⟩ Oriented Organic−Inorganic Perovskite Compound Stabilized by N (3 Aminopropyl)Imidazole with Im proved Optical Properties. *Chem. Mater.* **2006**, *18* (15), 3463−3469.
(21) Dohner, E. R.; Hoke, E. T.; Karunadasa, H. I. Self Assembly of Broadband White Light Emitters. *J. Am. Chem. Soc.* **2014**, *136* (5), 1718−1721.
(22) Dohner, E. R.; Jaffe, A.; Bradshaw, L. R.; Karunadasa, H. I. Intrinsic White Light Emission from Layered Hybrid Perovskites. *J. Am. Chem. Soc.* **2014**, *136* (38), 13154−13157.
(23) Yangui, A.; Garrot, D.; Lauret, J. S.; Lusson, A.; Bouchez, G.; Deleporte, E.; Pillet, S.; Bendeif, E. E.; Castro, M.; Triki, S.; et al. Optical Investigation of Broadband White Light Emission in Self Assembled Organic−Inorganic Perovskite $(C_6H_{11}\ NH_3)_2\ PbBr_4$. *J. Phys. Chem. C* **2015**, *119* (41), 23638−23647.
(24) Yuan, Z.; Zhou, C.; Messier, J.; Tian, Y.; Shu, Y.; Wang, J.; Xin, Y.; Ma, B. A Microscale Perovskite as Single Component Broadband Phosphor for Downconversion White Light Emitting Devices. *Adv. Opt. Mater.* **2016**, *4* (12), 2009−2015.
(25) Yangui, A.; Pillet, S.; Lusson, A.; Bendeif, E. E.; Triki, S.; Abid, Y.; Boukheddaden, K. Control of the White Light Emission in the Mixed Two Dimensional Hybrid Perovskites (C6H11NH3)2 [PbBr4−xIx. *J. Alloys Compd.* **2017**, *699*, 1122−1133.
(26) Mao, L.; Wu, Y.; Stoumpos, C. C.; Wasielewski, M. R.; Kanatzidis, M. G. White Light Emission and Structural Distortion in New Corrugated Two Dimensional Lead Bromide Perovskites. *J. Am. Chem. Soc.* **2017**, *139* (14), 5210−5215.
(27) Neogi, I.; Bruno, A.; Bahulayan, D.; Goh, T. W.; Ghosh, B.; Ganguly, R.; Cortecchia, D.; Sum, T. C.; Soci, C.; Mathews, N.; et al. Broadband Emitting 2 D Hybrid Organic Inorganic Perovskite Based on Cyclohexane Bis(Methylamonium) Cation. *ChemSusChem* **2017**, *10* (19), 3765−3772.
(28) Wang, M. S.; Guo, G. C. Inorganic−Organic Hybrid White Light Phosphors. *Chem. Commun.* **2016**, *52* (90), 13194−13204.
(29) Booker, E. P.; Thomas, T. H.; Quarti, C.; Stanton, M. R.; Dashwood, C. D.; Gillett, A. J.; Richter, J. M.; Pearson, A. J.; Davis, N. J. L. K.; Sirringhaus, H.; et al. Formation of Long Lived Color Centers for Broadband Visible Light Emission in Low Dimensional Layered Perovskites. *J. Am. Chem. Soc.* **2017**, *139* (51), 18632−18639.
(30) Dammak, T.; Fourati, N.; Boughzala, H.; Mlayah, A.; Abid, Y. X Ray Diffraction, Vibrational and Photoluminescence Studies of the Self Organized Quantum Well Crystal H3N(CH2)6NH3PbBr4. *J. Lumin.* **2007**, *127* (2), 404−408.
(31) Liu, G.; Kong, L.; Guo, P.; Stoumpos, C. C.; Hu, Q.; Liu, Z.; Cai, Z.; Gosztola, D. J.; Mao, H.; Kanatzidis, M. G.; et al. Two Regimes of Bandgap Red Shift and Partial Ambient Retention in PressureTreated Two Dimensional Perovskites. *ACS Energy Lett.* **2017**, *2* (11), 2518−2524.
(32) Cortecchia, D.; Yin, J.; Bruno, A.; Lo, S. Z. A.; Gurzadyan, G. G.; Mhaisalkar, S.; Bredas, J. L.; Soci, C. Polaron Self Localization in White Light Emitting Hybrid Perovskites. *J. Mater. Chem. C* **2017**, *5* (11), 2771−2780.
(33) Yin, J.; Li, H.; Cortecchia, D.; Soci, C.; Brédas, J. L. Excitonic and Polaronic Properties of 2D Hybrid Organic−Inorganic Perov skites. *ACS Energy Lett.* **2017**, *2* (2), 417−423.
(34) Wang, X.; Meng, W.; Liao, W.; Wang, J.; Xiong, R. G.; Yan, Y. Atomistic Mechanism of Broadband Emission in Metal Halide Perovskites. *J. Phys. Chem. Lett.* **2019**, *10*, 501−506.
(35) Cortecchia, D.; Neutzner, S.; Srimath Kandada, A. R.; Mosconi, E.; Meggiolaro, D.; De Angelis, F.; Soci, C.; Petrozza, A. Broadband Emission in Two Dimensional Hybrid Perovskites: The Role of Structural Deformation. *J. Am. Chem. Soc.* **2017**, *139* (1), 39−42.
(36) Dolomanov, O. V.; Bourhis, L. J.; Gildea, R. J.; Howard, J. a. K.; Puschmann, H. OLEX2: A Complete Structure Solution, Refinement and Analysis Program. *J. Appl. Crystallogr.* **2009**, *42* (2), 339−341.
(37) Sheldrick, G. M. A Short History of SHELX. *Acta Crystallogr., Sect. A: Found. Crystallogr.* **2008**, *64* (1), 112−122.
(38) Sheldrick, G. M. Crystal Structure Refinement with SHELXL. *Acta Crystallogr., Sect. C: Struct. Chem.* **2015**, *71* (1), 3−8.
(39) Lebedkin, S.; Blum, C.; Stürzl, N.; Hennrich, F.; Kappes, M. M. A Low Wavenumber Extended Confocal Raman Microscope with Very High Laser Excitation Line Discrimination. *Rev. Sci. Instrum.* **2011**, *82* (1), No. 013705.